Electronic Supplementary Information for:

The Effect of Counterions on the Formation and Structures of Ce(III) and Er(III) Chloranilate Frameworks

Katherine Bondaruk and Carol Hua*

School of Chemistry, The University of Melbourne, Parkville, Victoria, 3010, Australia. *E-mail: carol.hua@unimelb.edu.au

Table of Contents

Table S1. Crystallographic parameters for the 2D (6,3) honeycomb frameworks obtained in this study

	$[Ce_2(can)_3(H_2O)_6]\cdot 2H_2O \cdot 3C_3H_6O$ (1)	**$0.5[Er_2(can)_3(H_2O)_6]\cdot 2H_2O\cdot 1.5\ C_3H_6O$ (2)**
Formula	$C_{27}H_{38}Ce_2Cl_6O_{25}$	$C_{14}H_{20}Cl_3ErO_{13}$
M/g mol^{-1}	1255.51	669.91
Temperature (K)	100(2)	100(2)
Crystal system	Orthorhombic	Triclinic
Space Group	*Pbcm* (#57)	*P*-1 (#2)
Crystal size (mm^3)	0.07 × 0.06 × 0.05	0.05 × 0.04 × 0.03
Crystal Colour	Purple	Purple
Crystal Habit	Block	Needle
a (Å)	13.4577(2)	10.1018(2)
b (Å)	26.9167(3)	10.1792(3)
c (Å)	12.3779(2)	11.7960(3)
α (°)	90	103.488(2)
β (°)	90	109.692(2)
γ (°)	90	101.082(2)
V (Å^3)	4483.73(11)	1060.83(5)
Z	4	2
ρ_{calc} (mg/mm^3)	1.860	2.097
Reflections collected	42286/4968 [R_{merge} = 0.0491]	35555/4469 [R_{merge} = 0.0594]
Data/parameters	4444/369	4292/319
Final R indexes [all data]	R_1 = 0.0307, wR_2 = 0.0849	R_1 = 0.0385, wR_2 = 0.1054
Goodness-of-fit on F^2	1.127	1.068

Table S2. Crystallographic parameters for the 3D diamond frameworks obtained in this study

	(DPMP)[Ce(can)$_2$(H$_2$O)]·H$_2$O·C$_3$H$_6$O (3)	**(DPMP)[Er(can)$_2$] (4)**	**(PPh$_4$)[Ce(can)$_2$(H$_2$O)] (5)**
Formula	$C_{33}H_{26}CeCl_4NO_{11}$	$C_{12}Cl_4ErO_8$	$C_{36}H_{22}CeCl_4O_9P$
M/g mol^{-1}	894.47	581.18	911.42
Temperature (K)	100(2)	100(2)	100(2)
Crystal system	Triclinic	Monoclinic	Monoclinic
Space Group	*P*-1 (#2)	*C*2/*c* (#15)	*C*2/*c* (#15)
Crystal size (mm^3)	0.05 × 0.04 × 0.02	0.2 × 0.15 × 0.1	0.1 × 0.05 × 0.03
Crystal Colour	Purple	Purple	Purple
Crystal Habit	Block	Prism	Prism
a (Å)	10.98110(10)	14.7203(2)	25.8876(2)
b (Å)	12.47830(10)	23.7156(2)	15.68090(10)
c (Å)	14.02530(10)	10.32950(10)	20.2420(2)
α (°)	102.3490(10)	90	90
β (°)	107.0440(10)	116.0680(10)	96.9340(10)
γ (°)	97.1940(10)	90	90
V (Å^3)	1758.20(3)	3239.20(7)	8156.96(12)
Z	2	4	8
ρ_{calc} (mg/mm^3)	1.690	1.192	1.160
Reflections collected	66223/7335 [R_{merge} = 0.0530]	39643/10292 [R_{merge} = 0.0250]	43074/8614 [R_{merge} = 0.0533]
Data/parameters	7119/457	9490/114	8211/456
Final R indexes [all data]	R_1 = 0.0298, wR_2 = 0.0750	R_1 = 0.0230, wR_2 = 0.0639	R_1 = 0.0360, wR_2 = 0.0948
Goodness-of-fit on F^2	1.112	1.059	1.052

Table S3. Crystallographic parameters for frameworks containing PPh_3Me^+ obtained in this study

	$(PPh_3Me)[Ce(can)_2(H_2O)]$ (6)	**$(PPh_3Me)_2[Er_2(can)_4]\cdot H_2O$ (7)**
Formula	$C_{93}H_{58}Ce_3Cl_{12}O_{27}P_3$	$C_{62}H_{36}Cl_8Er_2O_{17}P_2$
M/g mol^{-1}	2546.42	1732.97
Temperature (K)	100(2)	100(2)
Crystal system	Monoclinic	Monoclinic
Space Group	$P2_1/n$ (#14)	$P2_1/c$ (#14)
Crystal size (mm^3)	0.200 × 0.1 × 0.050	0.1 × 0.05 × 0.03
Crystal Colour	Purple	Purple
Crystal Habit	Prism	Blade
a (Å)	17.31600(10)	16.58380(10)
b (Å)	36.7219(2)	19.67230(10)
c (Å)	24.3429(15)	26.00730(10)
α (°)	90	90
β (°)	100.0320(10)	104.1510(10)
γ (°)	90	90
V (Å^3)	11606.33(12)	8227.19(8)
Z	4	4
ρ_{calc} (mg/mm^3)	1.457	1.399
Reflections collected	75029/23370 [R_{merge} = 0.0939]	131931/17466 [R_{merge} = 0.0751]
Data/parameters	19943/1363	16001/822
Final R indexes [all data]	R_1 = 0.0668, wR_2 = 0.1922	R_1 = 0.0379, wR_2 = 0.1054
Goodness-of-fit on F^2	1.044	1.046

Table S4. Analysis of the possible coordination geometries using the SHAPE program for the 9-coordinate Ce(III) containing structures, compounds **1**, **3** and **5**.

Geometry	Symmetry	1 (Ce1)	1 (Ce2)	3	5
EP-9	D_{9h}	36.593	36.972	36.546	36.619
OPY-9	C_{8v}	23.242	23.030	21.176	21.888
HBPY-9	D_{7h}	19.688	19.803	20.003	19.053
JTC-9	C_{3v}	15.740	16.037	14.865	16.156
JCCU-9	C_{4v}	10.781	11.107	11.180	9.732
CCU-9	C_{4v}	9.662	9.711	9.757	8.291
JCSAPR-9	C_{4v}	1.349	1.576	1.699	2.476
CSAPR-9	C_{4v}	**0.342**	**0.324**	**0.509**	1.275
JTCTPR-9	D_{3h}	3.048	3.279	3.253	2.628
TCTPR-9	D_{3h}	1.552	1.529	1.516	**0.843**
JTDIC-9	C_{3v}	12.378	12.373	11.958	11.835
HH-9	C_{2v}	12.074	12.076	12.582	10.974
MFF-9	C_s	0.966	0.923	1.231	1.688

EP-9 = Enneagon; OPY-9 = Octagonal pyramid; HBPY-9 = Heptagonal bipyramid; JTC-9 = Triangular cupola (J3) = trivacant cuboctahedron; JCCU-9 = Capped cube (Elongated square pyramid, J8); CCU-9 = Capped cube; JCSAPR-9 = Capped square antiprism (Gyroelongated square pyramid J10); CSAPR-9 = Capped square antiprism; JTCTPR-9 = Tricapped trigonal prism (J51); TCTPR-9 = Tricapped trigonal prism; JTDIC-9 = Tridiminished icosahedron (J63); HH-9 = Hula-hoop; MFF-9 = Muffin. The minima values are indicated in bold.

Table S5. Analysis of the possible coordination geometries using the SHAPE program for the 8-coordinate Er(III) containing structures, compounds **2**, **4** and **7**. Where more than one unique Er(III) exists, the analysis is shown for each of the Er(III) centres.

Geometry	Symmetry	2	4	7 (Er1)	7 (Er1)
OP-8	D_{8h}	26.747	29.260	30.430	29.564
HPY-8	C_{7v}	21.896	23.629	20.814	21.159
HBPY-8	D_{6h}	15.987	16.972	14.856	16.488
CU-8	O_h	14.505	9.913	17.277	12.198
SAPR-8	D_{4d}	4.791	**0.913**	9.679	2.280
TDD-8	D_{2d}	4.451	1.848	7.578	**2.242**
JGBF-8	D_{2d}	11.156	15.743	8.979	12.680
JETBPY-8	D_{3h}	25.877	26.555	24.471	24.064
JBTPR-8	C_{2v}	2.960	2.993	7.317	2.920
BTPR-8	C_{2v}	**1.850**	2.407	**6.085**	2.435
JSD-8	D_{2d}	5.700	4.531	9.336	3.736
TT-8	T_d	14.896	10.712	17.888	12.873
ETBPY-8	D_{3h}	21.110	21.124	18.839	20.475

OP-8 = Octagon; HPY-8 = Heptagonal pyramid; HBPY-8 = Hexagonal bipyramid; CU-8 = Cube; SAPR-8 = Square antiprism; TDD-8 = Triangular dodecahedron; JGBF-8 = Johnson gyrobifastigium J26; JETBPY-8 = Johnson elongated triangular bipyramid J14; JBTPR-8 = Biaugmented trigonal prism J50; BTPR-8 = Biaugmented trigonal prism; JSD-8 = Snub diphenoid J84; TT-8 = Triakis tetrahedron; ETBPY-8 = Elongated trigonal bipyramid. The minima values are indicated in bold.

Table S6. Analysis of the possible coordination geometries using the SHAPE program for the 9-coordinate Ce(III) centres in compound **6**.

Geometry	Symmetry	Ce1	Ce2	Ce3
EP-9	D_{9h}	37.088	36.275	36.790
OPY-9	C_{8v}	19.707	22.540	22.913
HBPY-9	D_{7h}	20.301	18.809	17.046
JTC-9	C_{3v}	16.060	15.805	14.887
JCCU-9	C_{4v}	11.677	10.267	7.255
CCU-9	C_{4v}	10.210	8.895	5.809
JCSAPR-9	C_{4v}	1.857	1.905	2.637
CSAPR-9	C_{4v}	**0.664**	**1.199**	1.643
JTCTPR-9	D_{3h}	3.438	3.535	3.187
TCTPR-9	D_{3h}	1.483	1.705	**1.539**
JTDIC-9	C_{3v}	11.844	11.874	12.066
HH-9	C_{2v}	12.853	9.941	9.429
MFF-9	C_s	1.034	**1.202**	1.652

EP-9 = Enneagon; OPY-9 = Octagonal pyramid; HBPY-9 = Heptagonal bipyramid; JTC-9 = Triangular cupola (J3) = trivacant cuboctahedron; JCCU-9 = Capped cube (Elongated square pyramid, J8); CCU-9 = Capped cube; JCSAPR-9 = Capped square antiprism (Gyroelongated square pyramid J10); CSAPR-9 = Capped square antiprism; JTCTPR-9 = Tricapped trigonal prism (J51); TCTPR-9 = Tricapped trigonal prism; JTDIC-9 = Tridiminished icosahedron (J63); HH-9 = Hula-hoop; MFF-9 = Muffin. The minima values are indicated in bold.

Figures

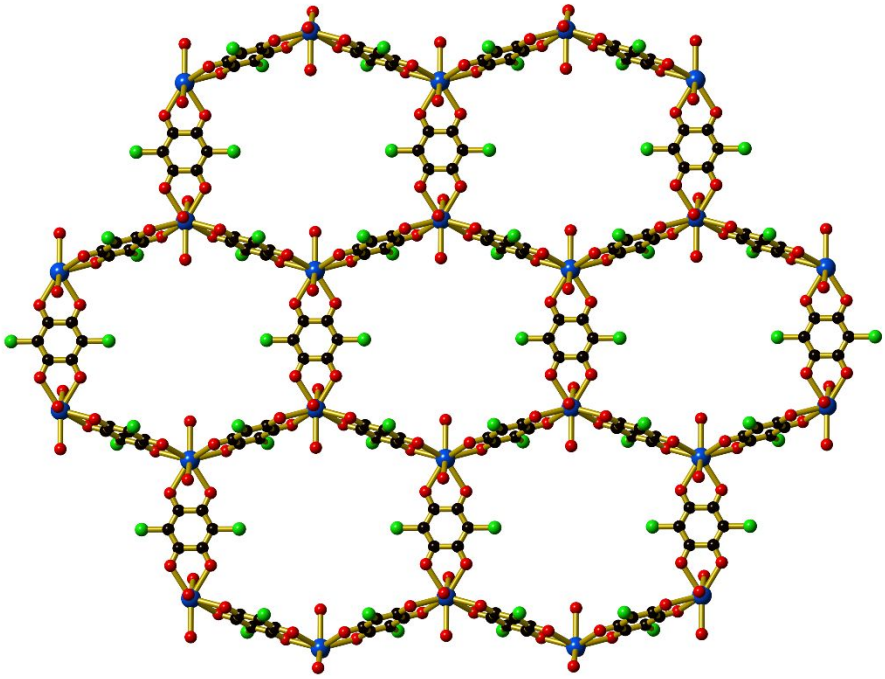

Figure S1. The (6,3) $[Ce_2(can)_3(H_2O)_6]$ network in $[Ce_2(can)_3(H_2O)_6]\cdot 12H_2O$[1, 2] with Ce(III) atoms located on parallel mirror planes perpendicular to the plane of the network. The $[Ce_2(can)_3(H_2O)_6]$ network in a second hydrated form, $[Ce_2(can)_3(H_2O)_6]\cdot 11H_2O$, which is formed upon exposure of the fully hydrated form to air, possesses a slightly distorted network with the absence of the mirror symmetry.

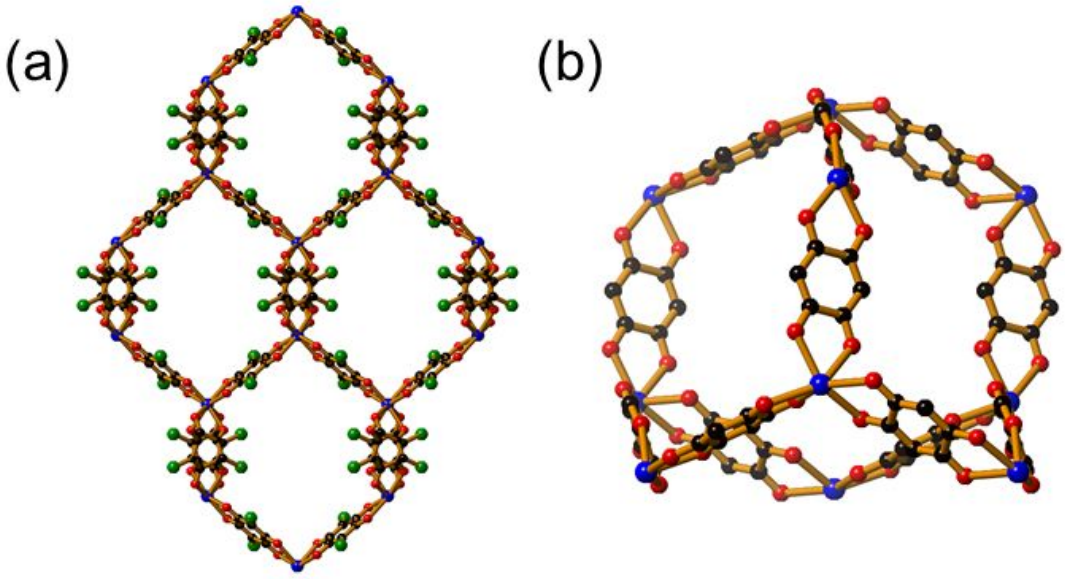

Figure S2. The 3D anionic framework, (DPMP)[Er(can)$_2$] (**4**) with **dia** topology depicting (a) the view along the *a* axis and (b) the distorted adamantane unit where the chlorines have been omitted for clarity. The hydrogens have been omitted for clarity and atoms are depicted as follows: carbon (black), erbium (dark blue), oxygen (red) and chlorine (green).

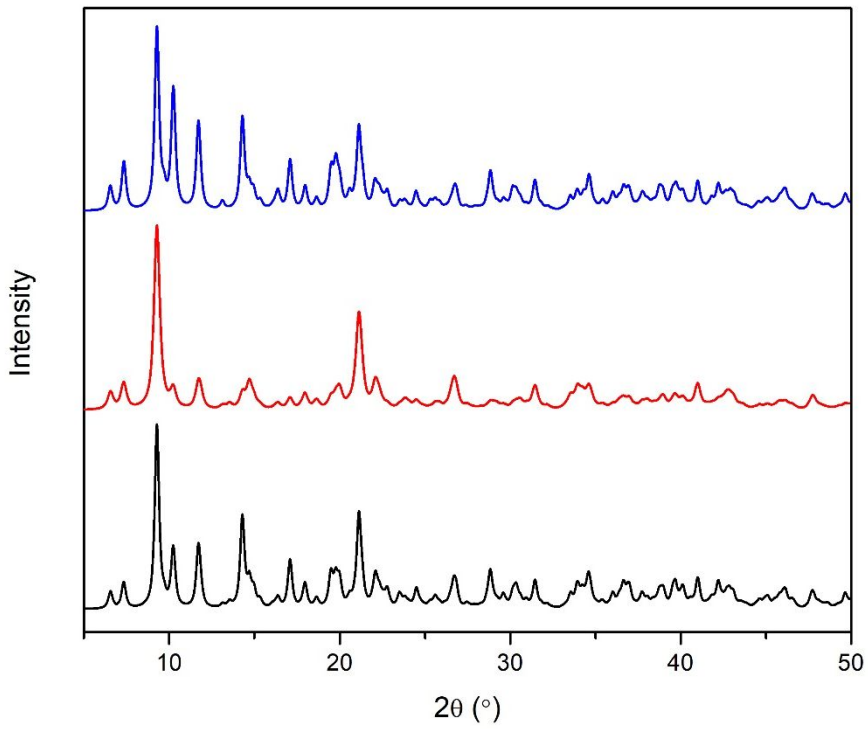

Figure S3. The calculated (black) and experimental powder XRD patterns of $[Ce_2(can)_3(H_2O)_6]\cdot 2H_2O\cdot 3C_3H_6O$ (**1**) with Bu_4N^+ (red) and Me_4N^+ (blue) cations.

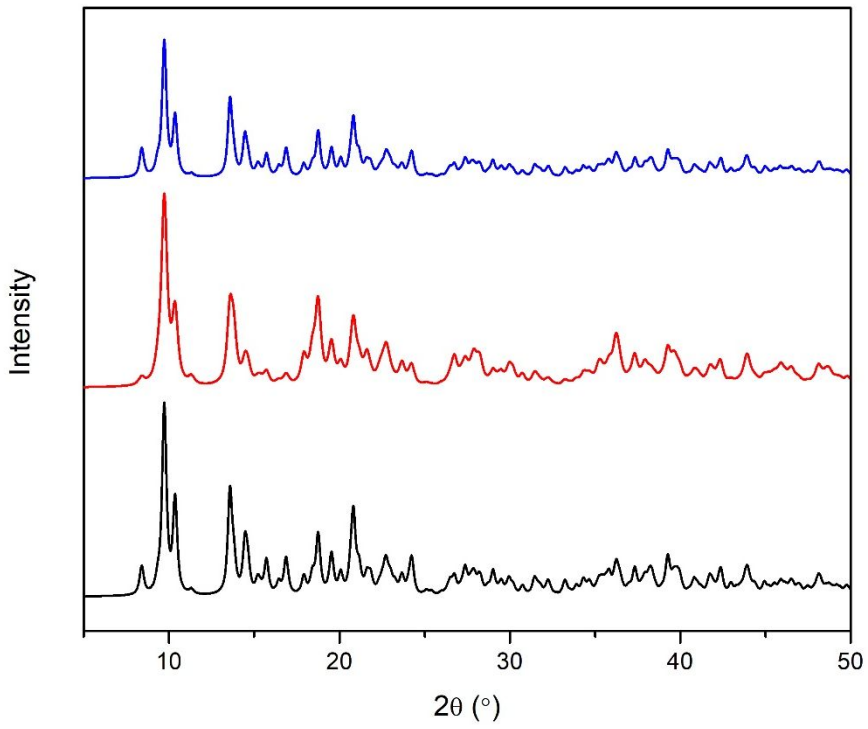

Figure S4. The calculated (black) and experimental powder XRD patterns of $[Er_2(can)_3(H_2O)_6]\cdot 2H_2O\cdot 1.5C_3H_6O$ (**2**) with Bu_4N^+ (red) and Me_4N^+ (blue) cations.

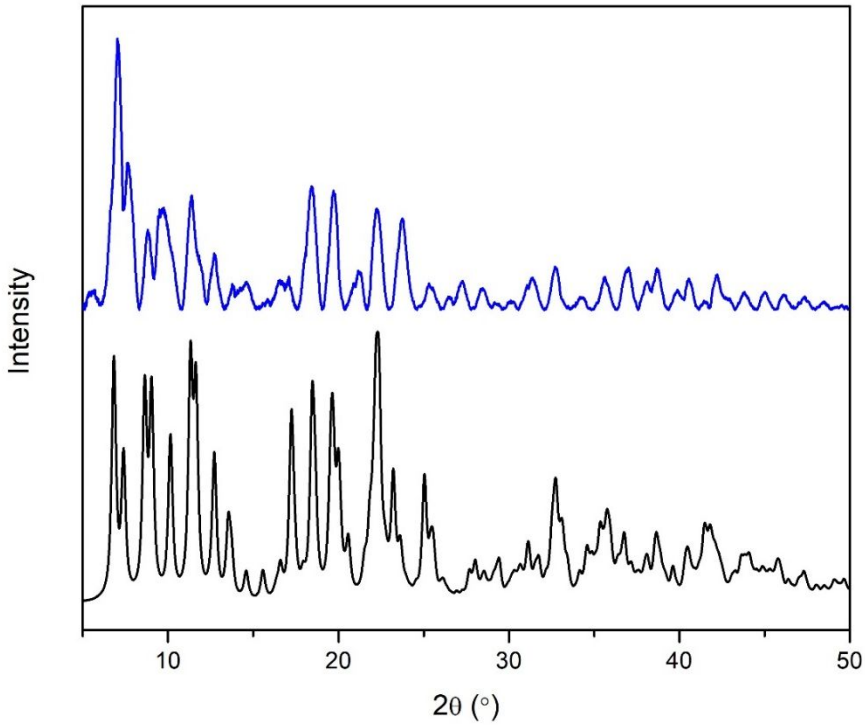

Figure S5. The experimental (blue) and calculated (black) powder XRD patterns of (DPMP)[Ce(can)$_2$(H_2O)]·H_2O·C_3H_6O (**3**).

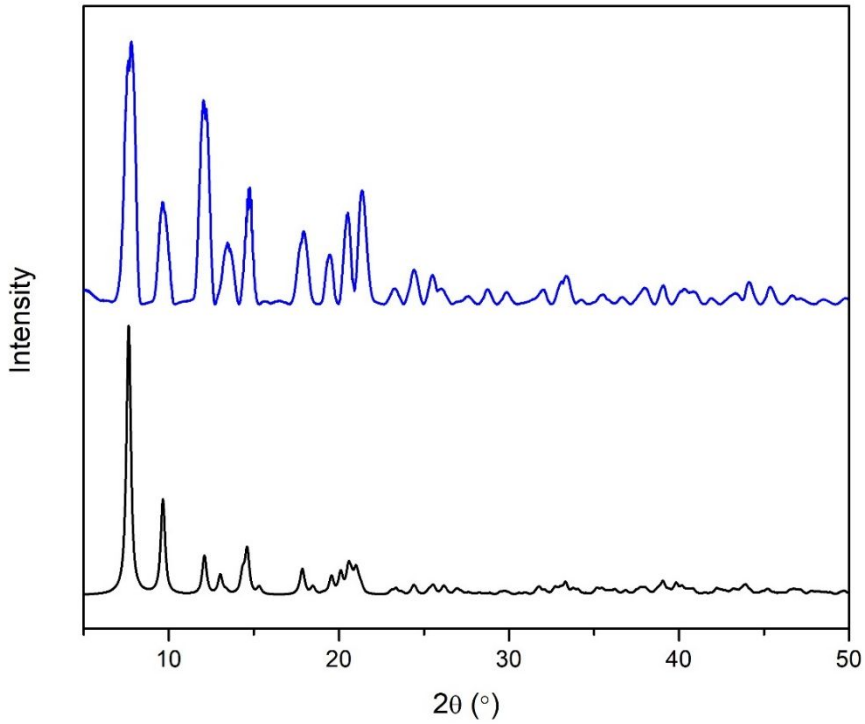

Figure S6. The experimental (blue) and calculated (black) powder XRD patterns of (DPMP)[Er(can)$_2$] (**4**).

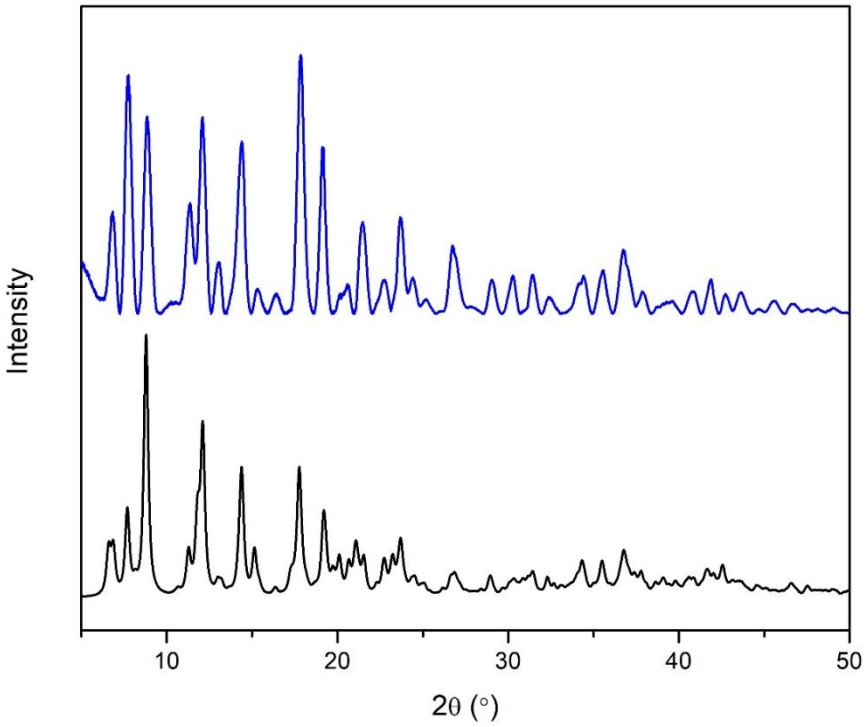

Figure S7. The experimental (blue) and calculated (black) powder XRD patterns of $(PPh_4)[Ce(can)_2(H_2O)]$ (**5**).

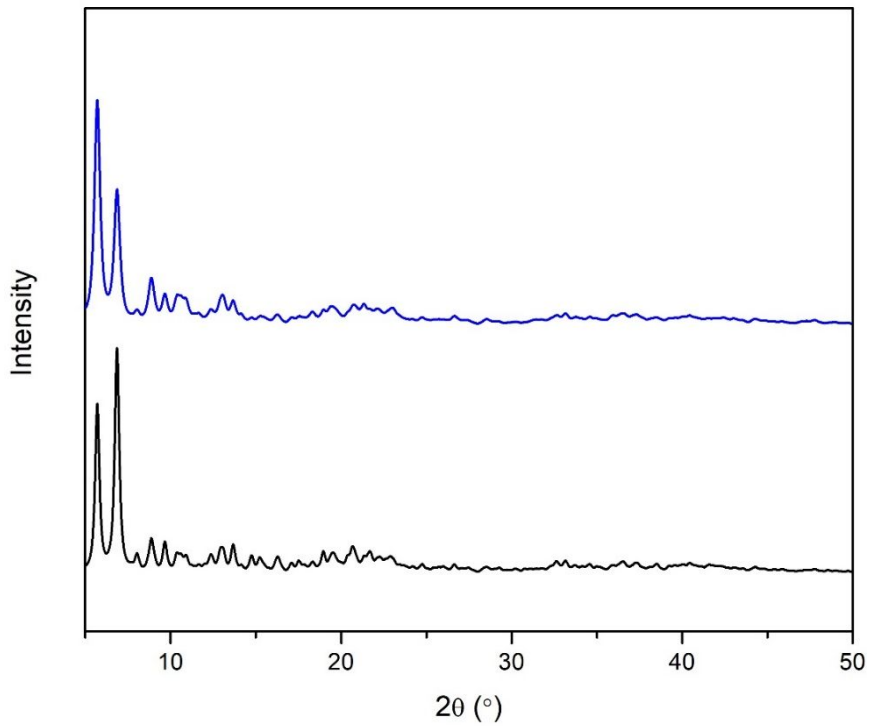

Figure S8. The experimental (blue) and calculated (black) powder XRD patterns of $(PPh_3Me)[Ce(can)_2(H_2O)]$ (**6**).

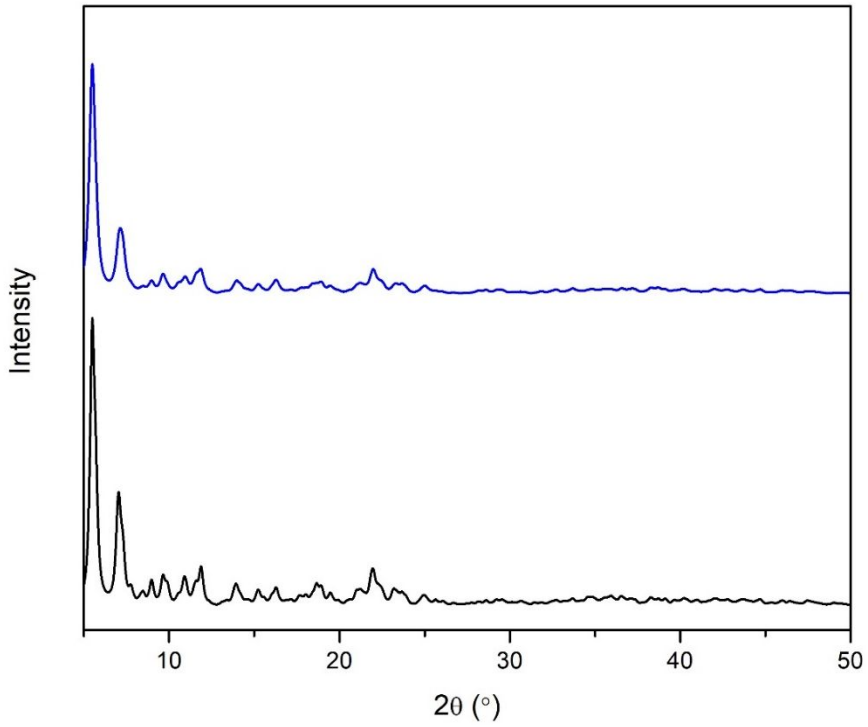

Figure S9. The experimental (blue) and calculated (black) powder XRD patterns of $(PPh_3Me)_2[Er_2(can)_4]\cdot H_2O$ (**7**).

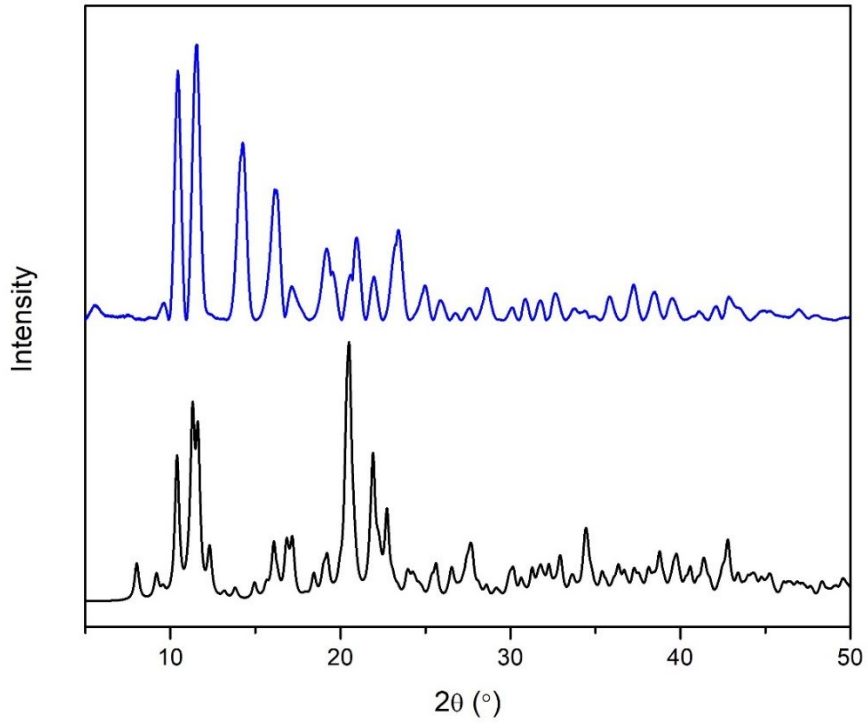

Figure S10. Powder XRD of the distorted 2D honeycomb $[Er_2(can)_3(H_2O)_6]$ formed upon the attempted synthesis of a diamond network with PPh_4^+ (blue) with the calculated (black) pattern from XAXBEG.[3]

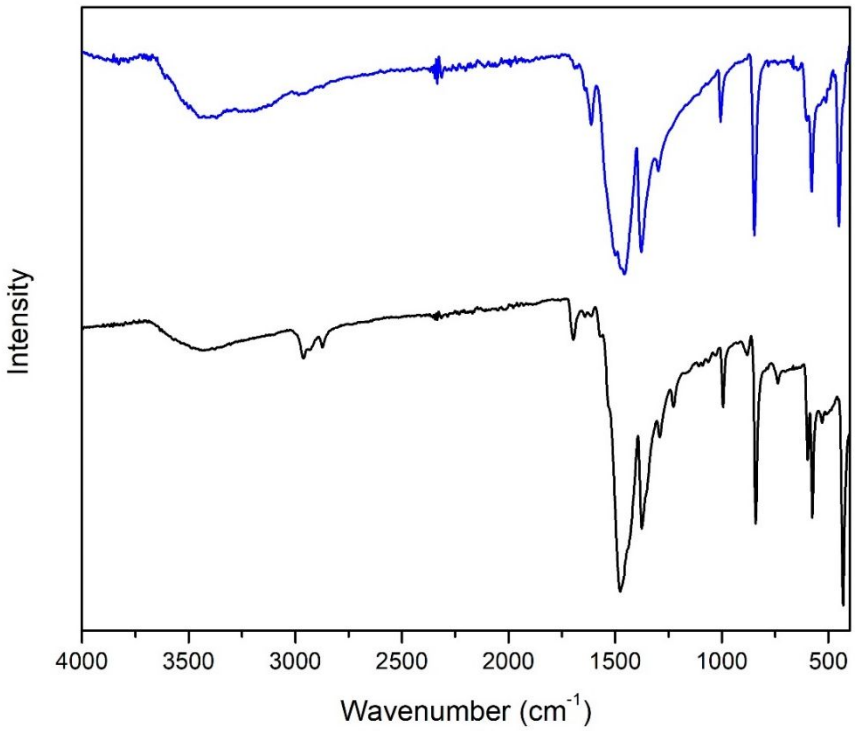

Figure S11. ATR-FTIR spectra of the neutral 2D (6,3) honeycomb frameworks, $[Ce_2(can)_3(H_2O)_6]\cdot 2H_2O\cdot 3C_3H_6O$ (**1**) (black) and $[Er_2(can)_3(H_2O)_6]\cdot 2H_2O\cdot 1.5C_3H_6O$ (**2**) (blue).

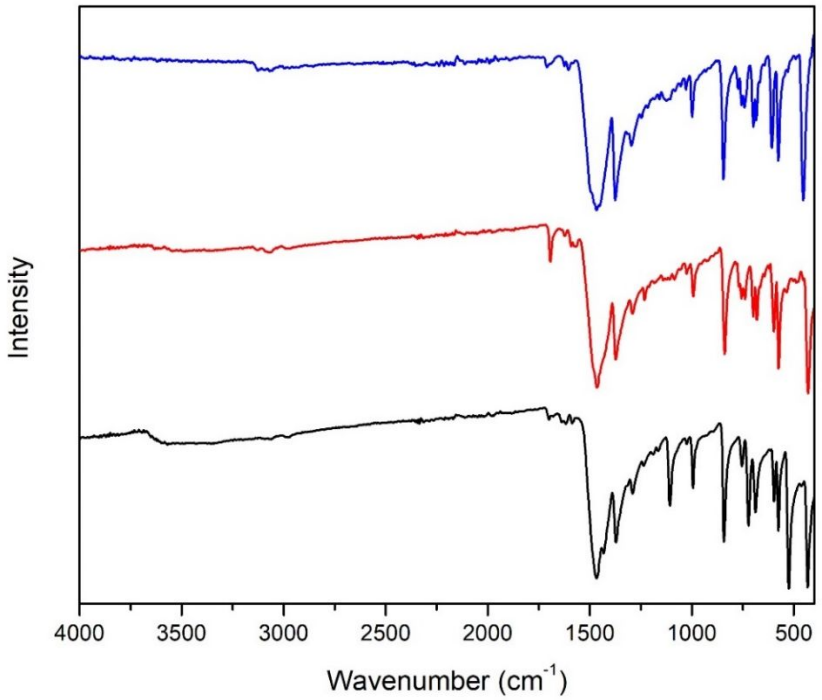

Figure S12. ATR-FTIR spectra of the anionic 3D diamond frameworks, $(DPMP)[Ce(can)_2(H_2O)]\cdot H_2O\cdot C_3H_6O$ (**3**) (red), $(DPMP)[Er(can)_2]$ (**4**) (blue) and $(PPh_4)[Ce(can)_2(H_2O)]$ (**5**) (black).

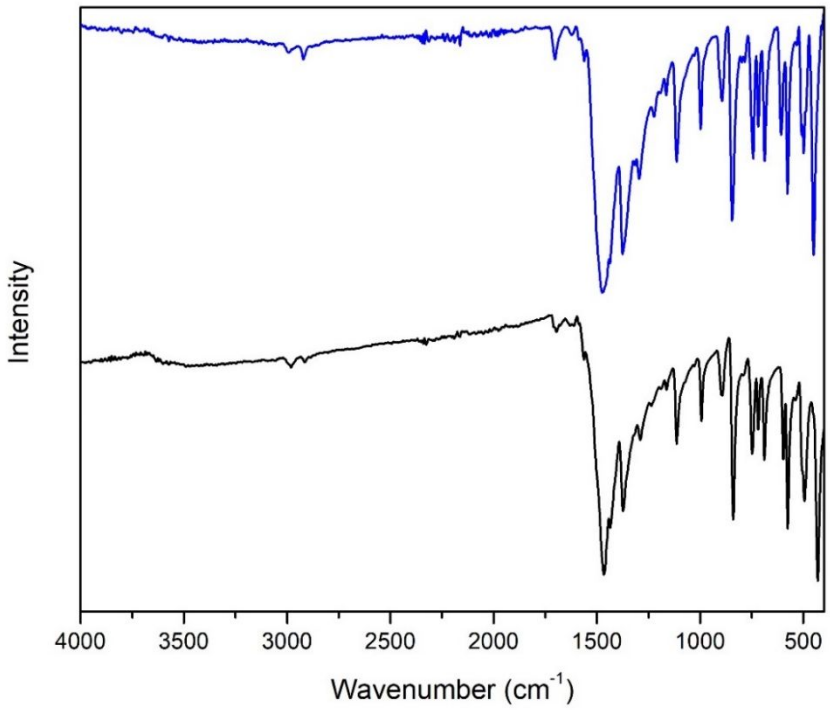

Figure S13. ATR-FTIR spectra of the anionic 3D frameworks with the PPh_3Me^+ cation, $(PPh_3Me)[Ce(can)_2(H_2O)]$ (**6**) (black) and $(PPh_3Me)_2[Er_2(can)_4]\cdot H_2O$ (**7**) (blue).

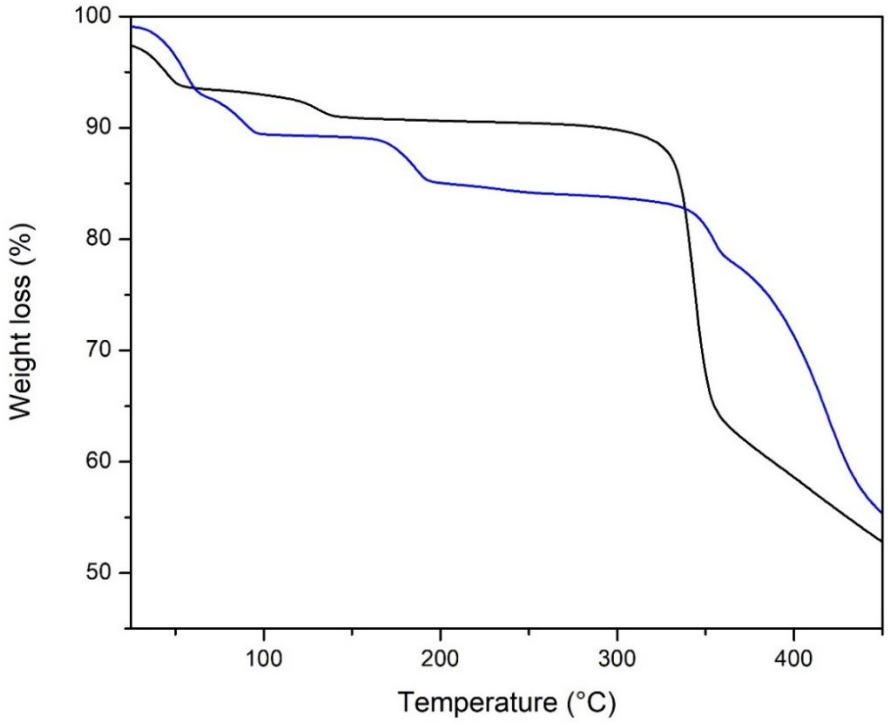

Figure S14. Thermal gravimetric analysis of neutral 2D (6,3) honeycomb frameworks, $[Ce_2(can)_3(H_2O)_6]\cdot 2H_2O\cdot 3C_3H_6O$ (**1**) (black) and $[Er_2(can)_3(H_2O)_6]\cdot 2H_2O\cdot 1.5C_3H_6O$ (**2**) (blue), from 25 to 450 °C.

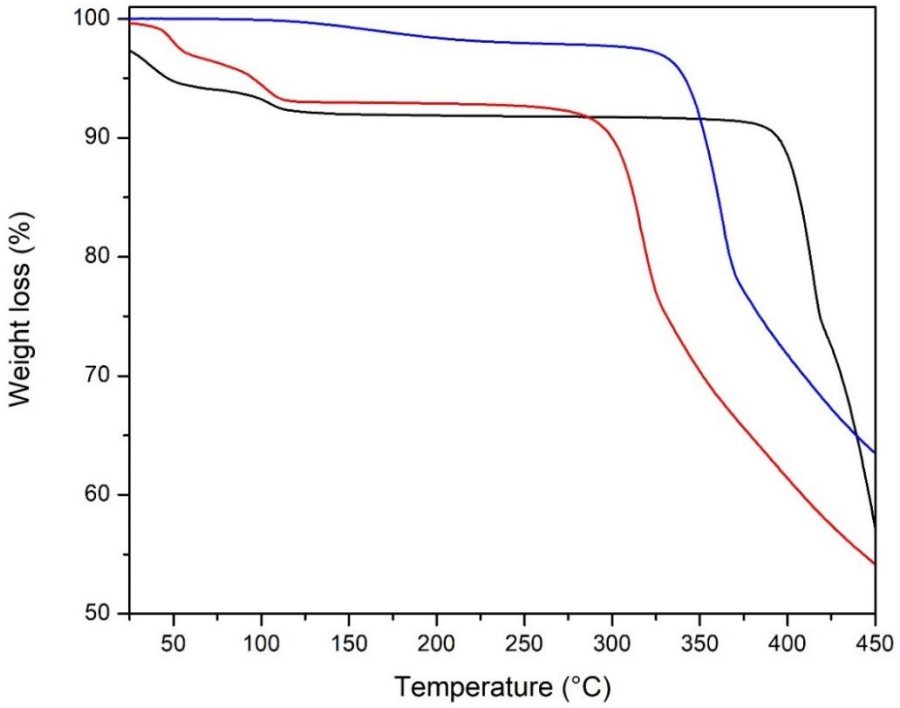

Figure S15. Thermal gravimetric analysis of the anionic 3D diamond frameworks, (DPMP)[Ce(can)$_2$(H$_2$O)]·H$_2$O·C$_3$H$_6$O (**3**) (black), (DPMP)[Er(can)$_2$] (**4**) (blue) and (PPh$_4$)[Ce(can)$_2$(H$_2$O)] (**5**) (red), from 25 to 450 °C.

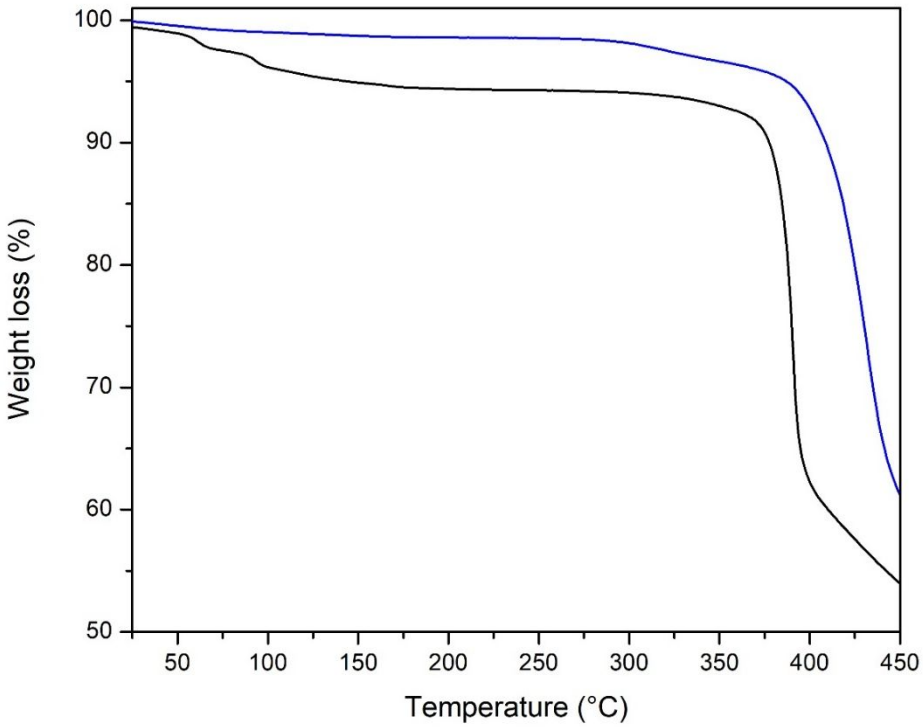

Figure S16. Thermal gravimetric analysis of the anionic 3D frameworks with the PPh_3Me^+ cation, (PPh_3Me)[Ce(can)$_2$(H$_2$O)] (**6**) (black) and (PPh_3Me)$_2$[Er$_2$(can)$_4$]·H$_2$O (**7**) (blue) from 25 to 450 °C.

References

1. Abrahams, B. F.; Coleiro, J.; Hoskins, B. F.; Robson, R., Gas hydrate-like pentagonal dodecahedral $M_2(H_2O)_{18}$ cages (M = lanthanide or Y) in 2,5-dihydroxybenzoquinone-derived coordination polymers. *Chem. Commun.* **1996**, 603-604.
2. Abrahams, B. F.; Coleiro, J.; Ha, K.; Hoskins, B. F.; Orchard, S. D.; Robson, R., Dihydroxybenzoquinone and chloranilic acid derivatives of rare earth metals. *J. Chem. Soc., Dalton Trans.* **2002**, 1586-1594.
3. Benmansour, S.; Pérez-Herráez, I.; López-Martínez, G.; Gómez García, C. J., Solvent-modulated structures in anilato-based 2D coordination polymers. *Polyhedron* **2017,** *135*, 17-25.